High Efficiency Single-Stage Flyback Micro Inverter with Energy Regenerative Snubber

Elyes Mbarek[1†], Hamed Balloumi[2††], Ferid Kourda[3†††]

[#]Université de Tunis El Manar, ENIT-L.S.E, BP 37, 1002 Tunis Ie Belvédère, Tunis, Tunisia

Abstract
A low-cost technique for improving the efficiency of a single-stage Flyback micro inverter is proposed in the paper. The proposed low cost technique for improving the efficiency is based on a simple nondissipative snubber, consisting of just a few passive elements. A turn-off snubber is needed to limit the peak voltage stress that can damage the main switch when the transistor is turned OFF. In this paper, Simulation and experimental evaluation of the energy regenerative snubber dedicated to the flyback micro-inverter in comparison with other common snubbers is presented, the modes of operation of the converter are discussed and analyzed and the design of the converter with the passive snubber is reviewed. Experimental results obtained from a lab prototype are presented as well.

Keywords: *Flyback micro inverter, LCDD snubber, RCD snubber, CCM, DCM, CCM*

1. Introduction

Solar energy systems based on photovoltaic cells are becoming more popular during the last few decades, due to environmental concerns, the increase of fossil fuel prices, and the need for more energy.
Many different converter topologies [1-2] have been proposed for the solar energy systems, in order to supply the power to the ac grid. The most recent technology of those solar energy systems are the ac-PV modules [7], among those, the single Flyback Current Source Inverter [7] provides many advantages due to its simplicity, such as increased reliability, low cost, galvanic isolation and simple control.
This dc-ac flyback inverter based on the dc-dc single flyback makes use of only one magnetic component to attain both the energy transfer and isolation [1-2].
The challenge in the design of the single flyback micro-inverter is handling the leakage inductance energy of the flyback transformer. However, when the main transistor is turned OFF the high leakage inductance of the transformer develops high voltage
spikes across the main switch and can cause its destruction. Many different varieties of turn-off simple snubbers were reported in order to limit the rate of rise voltage across the switch, such as the dissipative RCD snubbers and the nondissipative LCDD snubbers. The conventional RCD snubber is simple, but the power stored in snubber capacitor dissipates on the resistor, therefore the efficiency suffers.
Conventional RCD Snubber is a popular and simple circuit to limit the peak voltage stress [3-8]. However, the use of the RCD snubber dissipates all of the energy absorbed, as a result of this; the RCD snubber power loss is not insignificant. Consequently, the conventional RCD Snubber cannot meet the requirements of the high efficiency objective.
In order to improve the converter efficiency, various different methods have been proposed, including the use of the zero-voltage switching techniques (ZVS) with active snubbers [8-9], and zero-current switching techniques (ZCS) with active snubbers [10-11], and the use of the nondissipative LCDD snubbers [5-7].
The nondissipative *passive LCDD* snubber can improve the converter efficiency; nevertheless, as compared to the passive RCD snubber, regenerative *LCDD* snubber requires an additional inductor that increases the component count and cost. Compared to RCD snubber that dissipates leakage energy in the resistance, regenerative LCDD snubber recovers leakage energy to the primary side of the single Flyback micro inverter improving the efficiency.
In this paper, design and optimization of regenerative LCDD snubber is presented. An experimental prototype is built to verify the theoretical findings. Experimental evaluation of the energy regenerative LCDD snubber in comparison with the Conventional RCD Snubber is presented in order to verify the theoretical and simulated findings.

2. Flyback micro inverter

2.1 Proposed micro inverter

The flyback microinverter, as shown in Fig. 1, performs energy flow from the DC side to the AC grid side. Flyback microinverter includes: a high frequency transformer with three windings, one primary and two inversed secondary windings, A primary switch Sp, and two secondary switches placed in each secondary winding S1 and S2. While the main semiconductor Sp is modulated in high frequency, the

Manuscript received March 5, 2022
Manuscript revised March 20, 2022
https://doi.org/10.22937/IJCSNS.2022.22.3.98

secondary switches are modulated in grid frequency (50 Hz), and each of them transfers energy to AC grid side during a half switching cycle. The LC filter is used to filter the current of the secondary grid side. The control bloc of the Flyback microinverter is based on a grid voltage sensor and the phase locked loop generates grid reference signal. The control algorithm bloc generates gates signals of Sp, S1 and S2 switches. A maximum power point extractor MPPT bloc calculates the reference duty cycle Dpk to extract the maximum power from the PV.

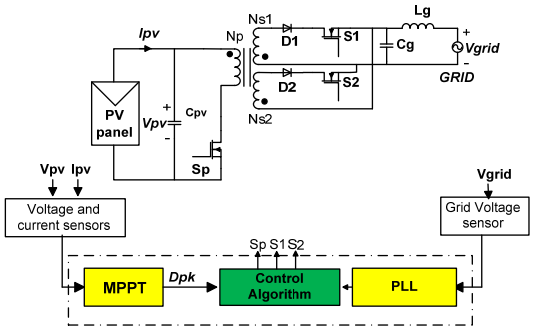

Fig. 1 Proposed Flyback microinverter

2.2 Operation modes of flyback micro inverter

The switching cycle begins with the turning on of the primary switch Sp (fig.2a). When the primary current in the primary winding ip of transformer increases, energy coming from the solar PV panel is stored in the magnetizing inductance L_m of the transformer. When the primary switch S_p is turned off, the stored energy in the transformer is transferred to the grid through the output rectifier D_1 and the controlled secondary switch S_1 (fig.2b) if the grid voltage V_{grid} is positive else stored energy is transferred to the grid, through the output rectifier D_2 and secondary switch S_2 (fig.2c) when grid voltage Vgrid is negative. typical waveforms for a switching cycle and controls signals are shown in Fig.3

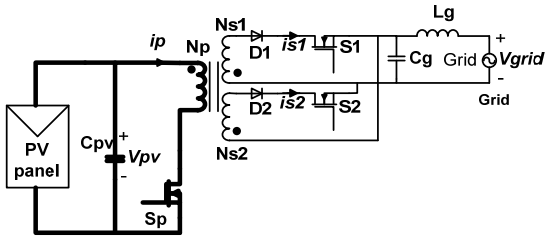

(a)

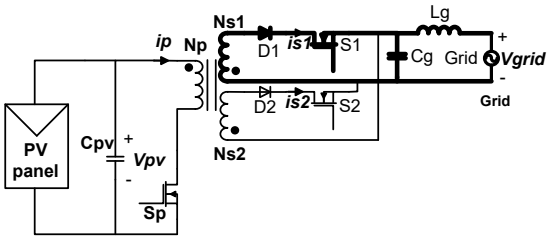

(b)

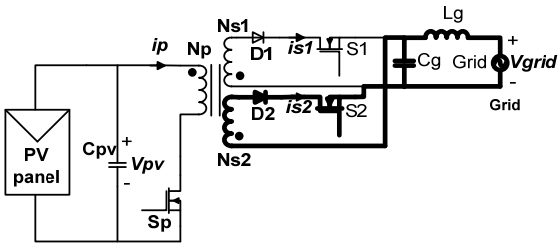

(c)

Fig.2 operating modes

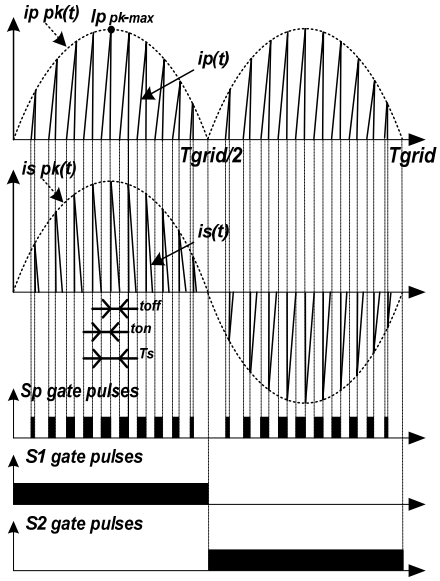

Fig. 3 Typical operating waveforms

3. Main converter design

In this section, the design of the proposed flyback microinverter is discussed in the DCM conduction mode. The design of the flyback microinverter can be split into two parts. For the first part, the design of the main converter is studied without considering the effect of leakage inductances L_k of the transformer and the snubber circuit. The magnetizing inductance L_m of the transformer is the most important component. The value of the magnetizing inductance L_m specifies the primary peak current ip_{pk}. If the

magnetizing inductance L_m is chosen too low, the pic primary current ip_{pk} will increase the stress on the primary switch Sp else if L_m is chosen too high the current may move toward to the CCM conduction mode.
For each switching cycle Ts (fig.3), a sufficient time t_{off} must be allowed to the magnetizing current in the transformer to fall to zero from its peak value, after the primary switch Sp has been turned off.The worst case to be studied is when the converter operates at its maximum duty cycle D_{pk} and the primary current reaches its maximum $ip_{pk\text{-}max}$ value as shown in Fig.3
Operating in the DCM conduction mode, $t_{off\text{-}pk}$ can be expressed as

$$toff_{pk} \leq Ts - ton_{pk} \quad (1)$$

The maximum on time ton_{pk} can be expressed as:

$$ton_{pk} = Dpk.Ts = \frac{Dpk}{fs} \quad (2)$$

When the primary switch S_p is turned off, stored energy in the transformer is transferred to output throw the secondary winding. During this mode the output voltage across the secondary winding is reflected to the primary. it can be expressed as

$$Vgrid(t) = Vgrid_{pk}.\sin(wg.t) \quad (3)$$

The fall of the current in L_m can be expressed by

$$NVgrid(t) = Lm\frac{dip(t)}{dt} \quad (4)$$

So, $toff_{pk}$ can be deducted and can be expressed as:

$$toff_{pk} = Lm\frac{Ip_{pk\_max}}{N.Vgrid_{pk}} \quad (5)$$

the primary current Ip_{pk_max} can be expressed as:

$$Ip_{pk\_max} = \frac{Vpv.Dpk}{Lm.fs} \quad (7)$$

Substituting (7) equation into equation (4) gives,

$$toff_{pk} = \frac{Vpv.Dpk}{Vgrid_{pk}.fs.N} \quad (8)$$

From equation (8) it can be seen that t_{off_pk} is dependent on various parameters. The switching frequency fs is fixed however the peak duty cycle Dpk and the turns ratio N need to be chosen. Considering the expression for DCM operation given in equation (1) and substituting equation (8) to get,

$$\frac{Vpv\ D_{pk}}{Vgrid_{pk}.fs.N} \leq Ts - ton_{pk} \quad (9)$$

Dividing the both sides of equation (9) by ton_pk, to get,

$$\frac{Vpv}{Vgrid_{pk}.N} \leq (\frac{1}{Dpk} - 1) \quad (10)$$

From equation (10) the turns ration N can be expressed as:

$$N \geq \frac{Vpv}{Vgrid_{pk}}(\frac{1}{Dpk} - 1)^{-1} \quad (11)$$

And the peak duty cycle Dpk can be expressed as:

$$Dpk \leq \frac{1}{\frac{Vpv}{NVgrid_{pk}} + 1} \quad (12)$$

The next study is focused to determinate the value of magnetizing inductance L_m that can store sufficient energy to be fed to the grid, for a rated output power P_{grid}
Assuming that the converter is ideal and lossless so that input and output power are equal, the required magnetizing inductance Lm for a given required output power Po can be determined from the following equation: [3]

$$Lm = \frac{1}{2}\left(\frac{Vpv}{Vgrid_{pk}}\right)^2 \frac{Dpk^2.Vgrid_{rms}{}^2}{fs.Po} \quad (13)$$

4. Snubber design

When the primary switch S_p is turned off, a high-voltage spike occurs between drain and source pins of the primary switch S_p because of a resonance between the leakage inductor L_k of the transformer and the output capacitor C_{DS} of the primary switch Sp. The excessive voltage may lead to an eventual damage to the primary switch. Therefore, it is necessary to add an additional circuit to clamp the drain source voltage and protect the switch. In these parts two snubbers' circuits are discussed: RCD snubber and LCDD snubber.

4.1 RCD snubber design

The flyback microinverter with RCD snubber is shown in Fig. 4. The microinverter goes through several modes of operation during a switching cycle. Equivalent circuit diagrams of this converter that show the flow of the current during any specific mode are shown in Fig. 5. Typical

waveforms for a switching cycle are shown in Fig.6.The inverter's modes of operation are as follows:

Mode 1 [t_0, t_1]

At t = t_0, the primary switch Sp is turned on (fig.5a), the source voltage is impressed across the main transformer primary winding and energy starts to be stored in the transformer. At t=t_1 the primary current reaches his peak value Ip_{pk}

Mode 2 [t1, t2]

At t = t_1, the primary switch Sp is turned off. The leakage energy flows through the output capacitance C_{DS} and the snubber circuit (fig.5b). RCD snubber uses a capacitor C_{sn} to limit the spike voltage in the primary switch V_{sp} and the resistor R_{sn} to dissipate the leakage transformer energy.

Mode 3 [t2, t3]

At t = t_2, the transformer begins to be demagnetized. The diode that conducts depends on the polarity of the AC grid voltage Vgrid. If this voltage is positive, then S_1 is on and current flows through D_1 (fig.5c), if this voltage is negative, then S_2 is on and current flows through D_2 (fig.5c') . This mode ends when the secondary current goes to zero at t_3.

Mode 4 [t_3, t_4]

At t=t_4 the secondary current goes to zero (fig5.d), there is no reflected voltage across the primary of the transformer. Then, the magnetizing inductance L_m begins to resonate with the primary switch Capacitor C_{DS}. The voltage across the switch swings between V_{pv}±NVgrid . This mode ends when the primary switch S_p is turned on.

The slope of the current i_{sn} is as follows:

$$\frac{di_{sn}}{dt} = -\left(\frac{V_{csn} - NV_{grid}}{L_k}\right) \tag{14}$$

The time t_s is:

$$t_s = \frac{L_k}{V_{csn} - NV_{grid}}\, Ip_{pk} \tag{15}$$

The snubber capacitor voltage V_{csn} should be determined at the minimum input voltage and full-load condition. This voltage V_{csn} should be approximately 2 to 2.5 times of NVgrid. Very small voltage V_{csn} results in a severe loss in the snubber circuit.

The resistance R_{sn} is obtained by [13]:

$$R_{sn} = \frac{V_{csn}^2}{\frac{1}{2} L_k I_{pk}^2 \frac{V_{csn}}{V_{csn} - NV_{grid}}\, f_s} \tag{16}$$

The maximum ripple voltage of the snubber capacitor ΔV_{csn} is obtained as follows [13]:

$$\Delta V_{csn} = \frac{V_{csn}}{C_{sn} R_{sn} f_s} \tag{17}$$

Generally, 5~10% ripple is reasonable [13]. Therefore, the snubber capacitance is calculated using equation (17).

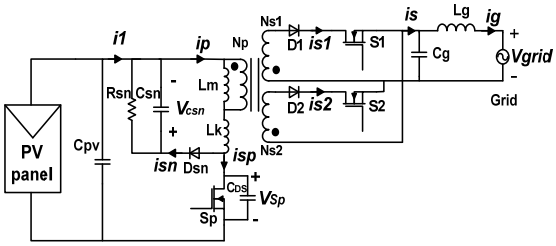

Fig.4 Flyback micro inverter with RCD snubber

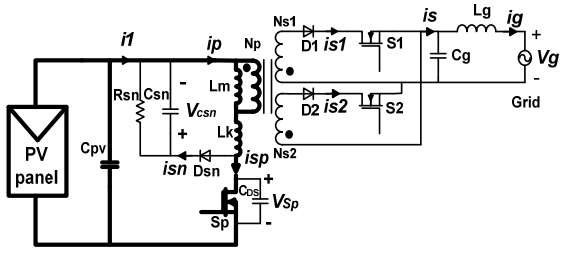

(a)

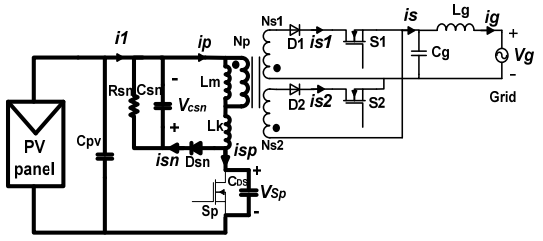

(b)

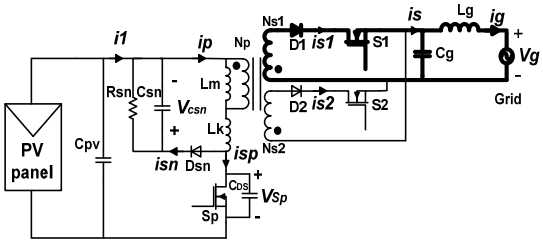

(c)

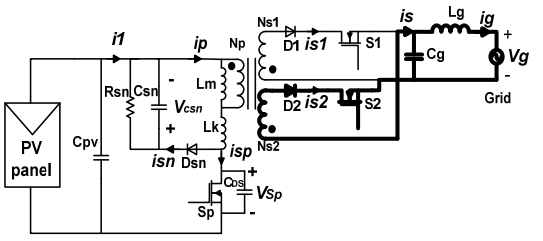

(c')

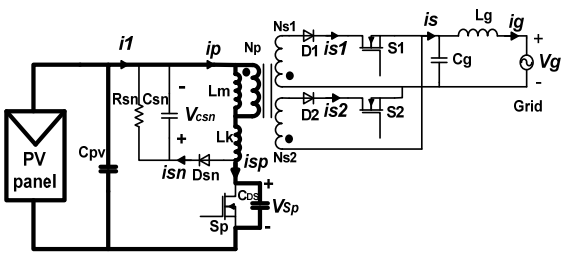

(d)

Fig. 5 Modes of operation

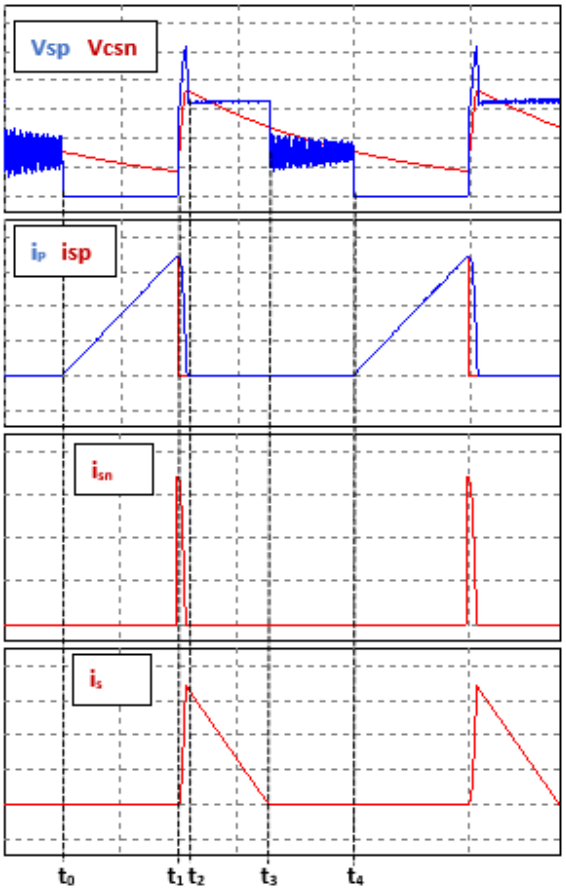

Fig.6 operating waveforms

4.2 Regenerative LCDD snubber design

The design method of the energy regenerative LCDD snubber has two goals, one is protecting the main switch Sp from the overvoltage stresses produced by the leakage inductor Lk and the other is improving the efficiency of this converter. Compared to RCD snubber that dissipates leakage energy, regenerative LCDD snubber recovers leakage energy to the primary side of the microinverter

The schematic diagram of the flyback microinverter with regenerative LCDD snubber is shown in Fig.7. This snubber is made of snubber diodes D_3 and D_4, snubber inductor L_s and snubber capacitor C_s.

The flyback microinverter goes through several modes of operation during a switching cycle. Equivalent circuit diagram for each mode of operation is shown Fig. 8 and typical waveforms are shown in Fig. 9. The modes of operation are as follows:

Mode 1 [t_0,t_1]

The switching cycle begins with the turning on of the main switch Sp at t = t_0 (fig.7a), the source voltage is impressed across the primary winding of transformer and energy starts to be stored in the transformer. At the same time the charged snubber capacitor C_s discharges through the main switch S_p and inductance L_s. The discharge mode concludes as the diode D_4 is turned off

Mode 2 [t_1,t_2]

When the capacitor C_{clamp} has been discharged (fig.7b) the transformer continues to be magnetizing due to the voltage impressed across the main transformer winding.

Mode 3 [t_2, t_3]

At t=t_2 the main switch Sp is turned off (fig.7c). The leakage energy stored in the transformer flows through two paths, one is through the output capacitance of Sp, C_{DS} and the other is through the snubber capacitor Cs and diode D_3.

At t=t_3, the voltage across the main switch V_{sp} is limited by the input voltage V_{pv}, the clamp capacitor voltage Vcs and the reflected instantaneous secondary AC voltage NVgrid

The voltage Vsp is given by

$$V_{sp} = V_{pv} + V_{cs} + NV_{grid} \quad (18)$$

Mode 4 [t_3, t_4]

At t = t_3, the transformer begins to be demagnetized. The diode that conducts depends on the polarity of the AC grid voltage Vgrid. If this voltage is positive, then S1 is on and current flows through D1(fig.7d); if this voltage is negative, then S2 is on and current flows through D2 (Figure). This mode ends when the secondary current goes to zero at t4.

As a result, stored energy in the snubber capacitor C_s discharges throw snubber inductor L_s, magnetizing inductance L_m and leakage L_k and returns to the primary capacitor C_{pv}. The discharge mode concludes when the diode D_4 is turned off.

Mode 5 [t_4, t_5]

During this mode the transformer continues to discharge through the secondary windings

Mode 6 [t_5,t_6]

This mode begins when the secondary current falls to zero at t=t_6, there is no reflected voltage across the primary of the transformer (fig.7f). As a result, the magnetizing inductance L_m begins to resonate with the capacitance of the primary switch C_{DS}. The voltage across the switch to swing

between Vpv ± NVgrid. This mode ends when switch S_p is turned on to start the next switching cycle.
The maximum value of V_{Sp}, reached during the off state of primary switch Sp, depends on the clamping voltage Vcs and on the input voltage Vpv:

$$V_{Sp} = V_{cs} + V_{pv} \tag{19}$$

Le snubber capacitor voltage is expressed by [14]:

$$V_{cs} = NV_{grid} + \sqrt{\frac{L_k I_{pk}^2}{C_s}} \tag{20}$$

the snubber capacitor Cs is obtained by [14]:

$$C_s = \frac{L_k I_{pk}^2}{\left(V_{Sp} - V_{pv} - NV_{grid}\right)^2} \tag{21}$$

The snubber inductor helps returning to primary the energy stored in Cs and also limits the peak current of the main switch during the polarity inversion of the voltage across Cs. This sets the limits of possible values for the inductance.
During the on time of the primary switch (Mode 1), energy stored in the capacitor snubber Cs is transferred to Ls throw primary switch Sp. therefore, this half period must be shorter than the minimum on time.
The upper limit for the inductance Ls can be calculated as [14]:

$$L_s = \left(\frac{D_{min}}{f_s \pi}\right)^2 \frac{1}{C_s} \tag{22}$$

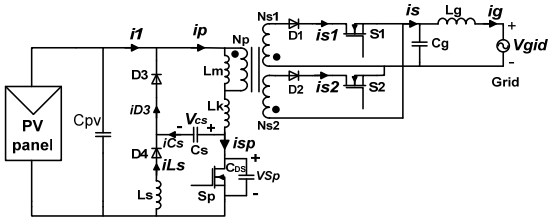

Fig.7 Flyback micro inverter with LCDD snubber

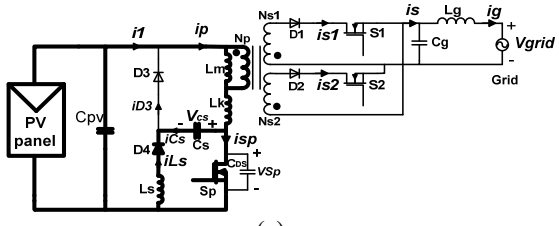

(a)

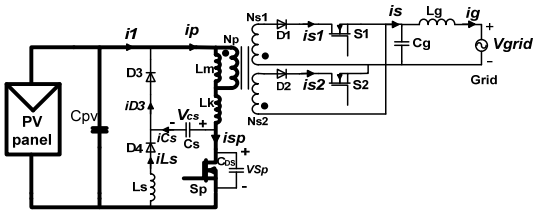

(b)

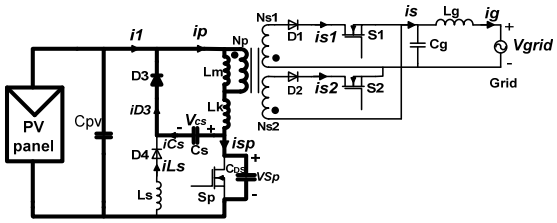

(c)

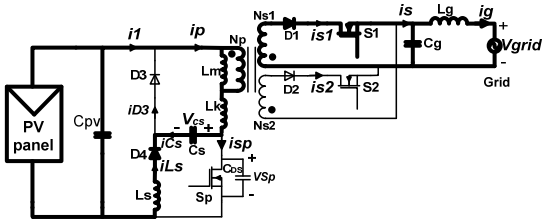

(d)

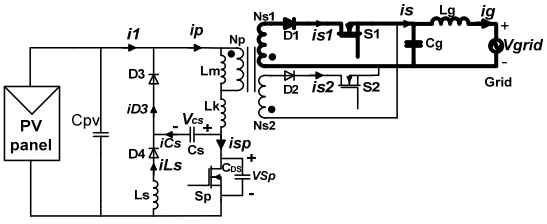

(e)

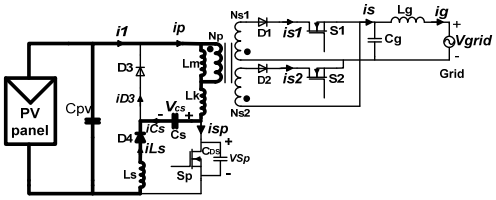

(f)

Fig.7 operating waveforms with LCDD snubber

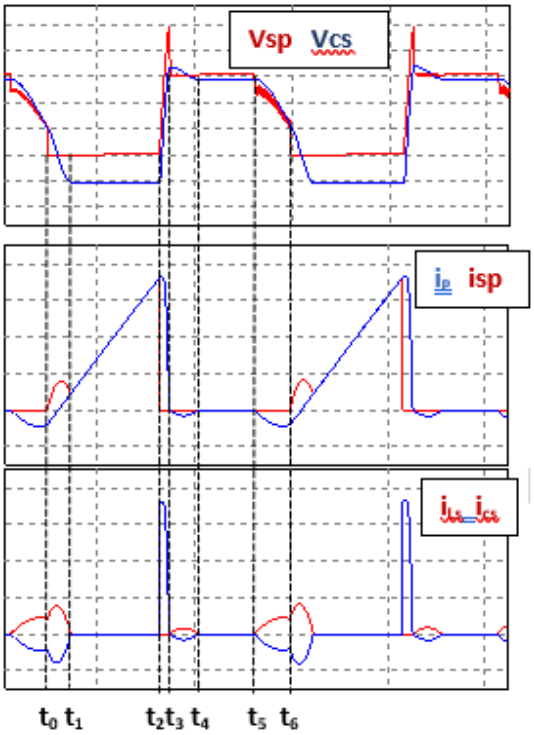

Fig .8: typical operating waveforms

4. Experimental results

To evaluate the proposed flyback microinverter, a 100W flyback micro inverter prototype was developed and tested as presented in Fig.9. The converter was supplied using a DC voltage source and STM32F407 DSP was used to generate the gating signals for the switches. The prototype was built using the two snubbers: RCD and regenerative LCDD snubber. The designed parameters of RCD and energy regenerative LCDD snubber are given in Table 1.

Figure 10 presents the output voltage and current injected to the grid for D_{pk}=0.3 using RCD snubber circuit (fig.10a) and LCDD snubber (fig.10b). From this figure it is clear that for the pic duty cycle D_{pk}, grid injected current grow using LCDD snubber.

Figure 11 presents voltage and current stress in the primary switch using RCD snubber when Dpk=0.3. The voltage stress in the primary switch Sp is limited to 76V and the current pic in the transformer reaches 10A when the primary switch turns off

Figure 12 presents voltage and current stress in the primary switch using LCDD snubber Dpk=0.3. The voltage stress in the primary switch Sp is limited to 68V and the current pic in the transformer reaches 5A.

For efficiency study, a comparison is made with the traditional RCD and the LCDD snubbers. The power efficiencies were measured on the same flyback microinverter prototype with different snubbers. The curves of the experimental efficiency of the two different snubbers under the same voltage stress are shown in Fig.13. It can be observed that the overall efficiency of energy regenerative LCDD snubber is about 10% higher than that of RCD snubbers

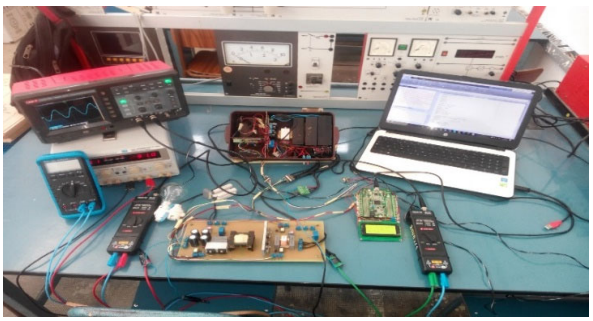

Figure 9. Prototype of a proposed flyback micro inverter

Table 1: The specifications and parameters of prototype with proposed topology.

Parameter	Value
Output power (Pout)	100W
DC voltage source	30V
Grid voltage (Vgrid)	230V-50Hz
Switching frequency (fs)	20Khz
Input capacitance (Cpv)	4mF
Primary switch (Sp)	FB4227
Secondaries switches (S1,S2)	IRFP460
Secondaries diodes (D1,D2)	BY229
Transformer	
Core type	ETD39
Turns ratio N	0.11
Magnetizing inductance Lm	36µH
Maximum flux density (Bm)	0.2T
RDC snubber	
Rsn	100Ω
Csn	330nF
LCDD snubber	
Ls	11µH
Cs	330nF

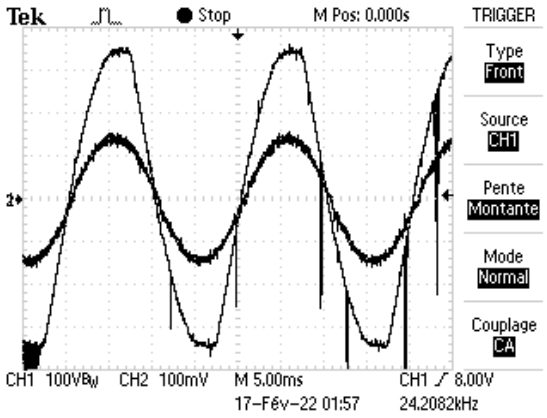

(a)

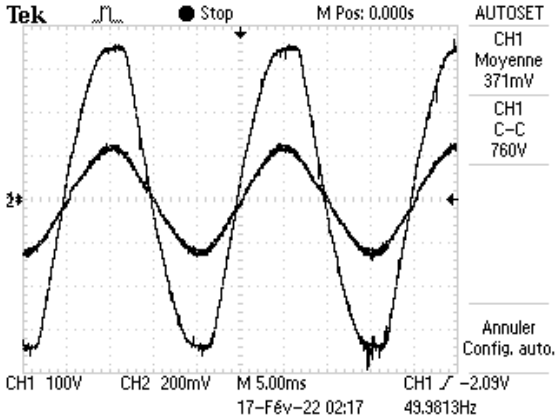

(b)

Figure 10. Grid voltage and current using different snubber Dpk=0.3

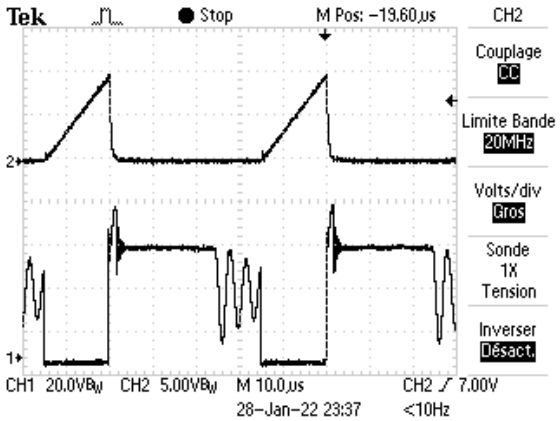

Figure 11. voltage and current stress in the primary switch using RCD snubber Dpk=0.3

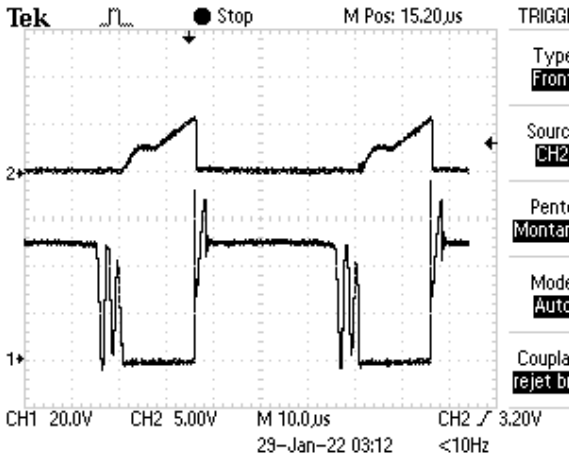

Figure 12. voltage and current stress in the primary switch using LCDD snubber Dpk=0.3

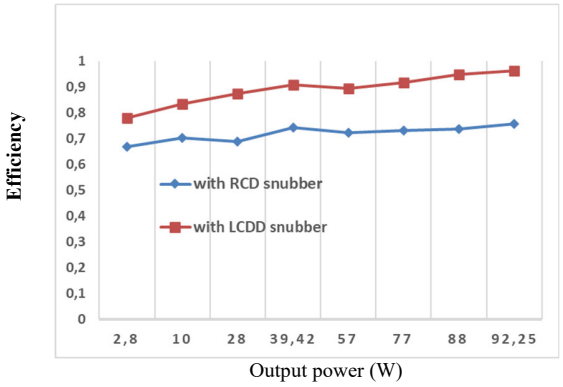

Figure 13. efficiency comparison

CONCLUSION

This paper examined the energy regenerating LCDD snubber suited for the flyback microinverter. Comparative experimental performance evaluation of this energy regenerative LCDD snubber was performed. From the experimental results, it is confirmed that this snubber has a better performance in total efficiency than those with the conventional RCD snubber. The experimental efficiency shows that under the same voltage stress the efficiency of energy regenerative snubber has 10% improvement in average over RCD snubber. A prototype was developed to show the correct operation of the proposed flyback microinverter. The experimental results demonstrate the effectiveness of the developed converter.

Acknowledgments

This work was supported by the Tunisian Ministry of High Education and Research under Grant LSE, ENIT, LR 11ES15.

References

[1]D. Meneses, F. Blaabjerg, O. Garcia and J. Cobos, "Review and comparison of step-up transformer less topologies for photovoltaic ac-module application," IEEE Trans. Power Electron., vol. 28, no. 6, pp. 2649 - 2662, Jun. 2013.

[2] T. Freddy, N. A. Rahim, W. P. Hew and H. S. Che, "Comparison and Analysis of Single-Phase Transformerless Grid-Connected PV Inverters," IEEE Trans. Power Electron., vol. 29, no. 10, pp. 5358 -5369, Oct. 2014.

[3] A. Ch. Kyritsis, E. C. Tatakis and N. P. Papanikolaou, "Optimum design of the current-source Flyback inverter for decentralized grid-connected photovoltaic systems," IEEE Trans. Energy Conv., vol.23, no.1, pp. 281-293, Mar. 2008.

[4] Z. Zhang, X.-F. He and Y.-F. Liu, "An optimal control method for photovoltaic grid-tied-interleaved Flyback micro inverters to achieve high efficiency in wide load range," IEEE Trans. Power Electron., vol. 28, no. 11, pp. 5074–5087, Nov. 2013.

[5] A. C. Nanakos, E. C. Tatakis and N. P. Papanikolaou, "A weighted-efficiency-oriented design methodology of flyback inverter for ac photovoltaic modules," IEEE Trans. Power Electron., vol. 27, no. 7, pp. 3221- 3233, Jul. 2012.

[6] H. Hu, S. Harb, N. H. Kutkut, Z. J. Shen and I. Batarseh, "A single-stage micro inverter without using eletrolytic capacitors," IEEE Trans. Power Electron., vol. 28, no. 6, pp. 2677–2687, Jun. 2013.

[7] Y. Li and R. Oruganti, "A Low Cost Flyback CCM Inverter for AC Module Application," IEEE Trans. Power Electron., vol. 27, no. 3, pp. 1295–1303, Mar. 2012.

[8] T. V. Thang, N. M. Thao, J.-H. Jang and J.-H. Park, "Analysis and design of grid-connected photovoltaic systems with multiple-integrated converters and a pseudo-dc-link inverter," IEEE Trans. Ind. Electron., vol.61, no. 7, pp. 3377–3386, Jul. 2014.

[9] F. F. Edwin, W. Xiao and V. Khadikar, "Dynamic modeling and control of interleaved flyback module integrated converter for PV power applications," IEEE Trans. Ind. Electron., vol. 61, no. 3, pp. 1377–1388,Mar. 2014.

[10] G. C. Christidis, A. C. Nanakos and E. C. Tatakis, "Hybrid Discontinuous/Boundary Conduction Mode of Flyback Microinverter for AC-PV Modules," IEEE Trans. Power Electron., vol. 31, no. 6, Jun. 2016.

[11] G. S. Dimitrakakis, E. C. Tatakis and E. J. Rikos, "A semiempirical model to determine HF copper losses in magnetic components with nonlayered coils," IEEE Trans. Power Electron., vol. 23, no. 6, pp. 2719-2728, Nov. 2008.

[12] K. Venkatachalam, C. R. Sullivan, T. Abdallah and H. Tacca, "Accurate prediction of ferrite core loss with non-sinusoidal waveforms using only Steinmetz parameters," Proc. IEEE Comput. Power Electron. Conf., 2002, pp. 36-41.

[13] Application Note AN-4147 "Design Guidelines for RCD Snubber of Flyback Converters"

[14] Esteban O. Lindstrom and Luciano A. Garcia-Rodriguez "Designing an Optimum Non-Dissipative LC Snubber for Step-Up Flyback Converters in DCM" IEEE 8th Latin American Symposium on Circuits & Systems (LASCAS) 2017

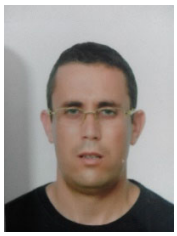

Elyes MBAREK received the M.S. degrees in Electrical Engineering from higher school of science and technology of Tunisia ESSTT in 2006, During 2006-2013, he designed switching power supplies in industry, he is currently working toward the Ph.D degree in renewable energy sources. His current research interests include power converters and renewable energy sources issues.